

Simultaneous 3-Nitrophenylhydrazine Derivatization Strategy of Carbonyl, Carboxyl and Phosphoryl Submetabolome for LC-MS/MS-Based Targeted Metabolomics with Improved Sensitivity and Coverage

Xiangjun Meng,¹ Huanhuan Pang,¹ Fei Sun, Xiaohan Jin, Bohong Wang, Ke Yao, LiAng Yao, Lijuan Wang, and Zeping Hu*



Cite This: *Anal. Chem.* 2021, 93, 10075–10083



Read Online

ACCESS |



Metrics & More

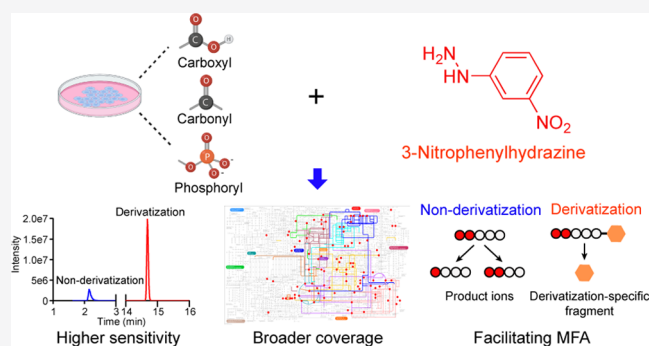


Article Recommendations



Supporting Information

ABSTRACT: Metabolomics is a powerful and essential technology for profiling metabolic phenotypes and exploring metabolic reprogramming, which enables the identification of biomarkers and provides mechanistic insights into physiology and disease. However, its applications are still limited by the technical challenges particularly in its detection sensitivity for the analysis of biological samples with limited amount, necessitating the development of highly sensitive approaches. Here, we developed a highly sensitive liquid chromatography tandem mass spectrometry method based on a 3-nitrophenylhydrazine (3-NPH) derivatization strategy that simultaneously targets carbonyl, carboxyl, and phosphoryl groups for targeted metabolomic analysis (HSD^{CP}-TM) in biological samples. By testing 130 endogenous metabolites including organic acids, amino acids, carbohydrates, nucleotides, carnitines, and vitamins, we showed that the derivatization strategy resulted in significantly improved detection sensitivity and chromatographic separation capability. Metabolic profiling of merely 60 oocytes and 5000 hematopoietic stem cells primarily isolated from mice demonstrated that this method enabled routine metabolomic analysis in trace amounts of biospecimens. Moreover, the derivatization strategy bypassed the tediousness of inferring the MS fragmentation patterns and simplified the complexity of monitoring ion pairs of metabolites, which greatly facilitated the metabolic flux analysis (MFA) for glycolysis, the tricarboxylic acid (TCA) cycle, and pentose phosphate pathway (PPP) in cell cultures. In summary, the novel 3-NPH derivatization-based method with high sensitivity, good chromatographic separation, and broad coverage showed great potential in promoting metabolomics and MFA, especially in trace amounts of biospecimens.



INTRODUCTION

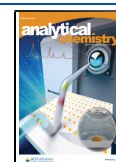
Metabolomics is a powerful tool for comprehensive metabolic profiling and precise metabolic phenotyping, which enables the identification of potential disease biomarkers and provides unique metabolic insights into the mechanisms of diseases.^{1,2} Despite the great advances achieved in both untargeted and targeted metabolomics, there still remain many technical challenges to be addressed.¹ The physicochemical diversity of metabolites makes it more difficult to develop methods with comprehensive coverage of the entire metabolome.^{3,4} Although untargeted metabolomics may detect more features than targeted methods do, the annotation and identification of the metabolites remain major challenges.^{5,6} The hydrophilic metabolites, such as amino acids, carbohydrates, and organic acids, account for a large proportion of the metabolome and play pivotal roles in many key metabolic processes.⁷ Chromatographically, hydrophilic metabolites are poorly

separated on the most commonly used reversed-phase liquid chromatography (LC) columns due to their poor retention.^{8–10} Moreover, the existence of isomeric metabolites, such as glucose and fructose, makes the separation even more challenging.¹¹ The co-elution of metabolites may also cause ion suppression, resulting in compromised detection sensitivity.¹² In addition, some functionally important metabolites, such as carbohydrates, are usually poorly ionized in MS due to the absence of ionizable functional groups, making them difficult to be detected.¹³ Consequently, most current metabolomics

Received: February 19, 2021

Accepted: July 2, 2021

Published: July 16, 2021



methods are not sufficiently sensitive to routinely cover a decent portion of the metabolome, especially when analyzing trace amounts of biospecimens, such as stem cells, developmental embryos, and rare immune cells.^{14–16} To break through this technical bottleneck, we developed a liquid chromatography tandem mass spectrometry (LC-MS/MS)-based targeted metabolomics method, which enabled routine metabolomic analysis in only 10 000 primarily isolated mouse hematopoietic stem cells (HSCs).¹⁵ In addition, this metabolomics method has been widely used in various metabolism studies, including cancer,^{17–23} infectious diseases,^{24,25} stem cells,²⁶ and cardiovascular diseases.^{27,28} Yet, further improvements in the sensitivity of the method are still needed to enable the coverage of more metabolites in even fewer amounts of biospecimens.

Chemical derivatization can improve the ionization efficiency and chromatographic separation of metabolites, thereby significantly enhancing the detection sensitivity and metabolome coverage of the liquid chromatography-mass spectrometry (LC-MS) method.^{4,29–32} However, one derivatization reagent usually reacts with only one specific chemical group,^{33–37} leading to limited coverage of the metabolome in currently reported derivatization-based LC-MS assays. To expand the coverage of the metabolome, previous studies classified metabolites into different submetabolomes according to their functional groups, divided the samples into four aliquots, and derivatized them using different reagents: dansylation for amines and phenols, base-activated dansylation for hydroxyls, DmPA bromide for carboxylic acids, and dansylhydrazine for carbonyl metabolites.⁴ However, this “divide-and-conquer” approach suffers from low-throughput and tedious operations, and it is impractical for studies with a limited amount of biospecimens. Therefore, the development of a derivatization strategy that can simultaneously target multiple functional groups will be greatly beneficial for metabolomic analysis.

Metabolites containing carbonyl and carboxyl groups play diverse and significant roles in many key metabolic processes.^{35,38,39} Phenylhydrazine derivatizing reagents are generally well suited for the derivatization of carbonyl and carboxyl-containing metabolites, resulting in excellent MS ionization efficiency and LC separation performance.^{40–45} In this study, we presented a 3-NPH derivatization-based metabolomics strategy that could simultaneously target carbonyl, carboxyl, and phosphoryl groups. To the best of our knowledge, this is the first study applying the phenylhydrazine reagent to derivatize phosphorylated metabolites, which play important roles in central carbon and energy metabolism.³⁸ Our 3-NPH-based three-group derivatization strategy enables simultaneous analysis of various classes of metabolites in a single LC-MS run, including amino acids, organic acids, carbohydrates, nucleotides, carnitines, and vitamins, covering major metabolic pathways such as glycolysis, the TCA cycle, and PPP. Importantly, this method achieves significantly higher sensitivity and broader coverage, which enables the precise analysis of metabolites in trace amounts of biospecimens. Moreover, the derivatization modified the MS fragmentation patterns of metabolites and thereby greatly facilitated the MFA for glycolysis, the TCA cycle, and PPP by reducing the complexity of monitored ion pairs.

METHODS AND MATERIALS

Chemical Reagents and Materials. LC-MS grade acetonitrile, methanol, and formic acid were purchased from Honeywell (Muskegon, MI). 3-NPH, 1-ethyl-3-(3-(dimethylamino)propyl)carbodiimide (EDC), and pyridine were purchased from Sigma-Aldrich (St. Louis, MO). LC-MS grade water was prepared using a Milli-Q System (Billerica, MA).

Preparation of the Mouse Oocytes and HSCs. Four-week-old mice were treated with 10 units of pregnant mares serum gonadotropin (PMSG) by intraperitoneal injection. The ovaries were harvested 48 h post injection and chopped to obtain germinal vesicle (GV)-stage oocytes. To collect metaphase II (MII)-stage oocytes, the mice were intraperitoneally injected with 10 units of human chorionic gonadotropin (HCG) 48 h after the injection of PMSG. MII-stage oocytes were isolated from the oviduct ampullae 16 h after HCG injection. Granular cells around GV and MII oocytes were removed by hyaluronidase, and zona pellucida were removed using acid Tyrode's solution. The GV and MII oocytes were then washed with M2 medium and saline and directly collected into 80% methanol aqueous solution.

Mouse HSCs were isolated by flow cytometry as described.⁴⁶ Briefly, mouse bone marrow cells were collected by crushing the femurs with a pestle and mortar in Hank's buffered salt solution at 4 °C. For isolation of HSCs, bone marrow cells were stained with c-kit-APC antibody and pre-enriched using magnetic beads conjugated to anti-c-kit antibodies before flow cytometry. c-kit⁺ cells were directly sorted into a precooled 80% methanol aqueous solution.

Preparation of HeLa Cells for MFA. Glucose 6-phosphate isomerase-wild type (GPI-WT, *n* = 5) and glucose 6-phosphate isomerase-knockout (GPI-KO, *n* = 5) HeLa cells were cultured in DMEM. For MFA, cells were washed twice with PBS and the medium was replaced with pyruvate- and glucose-free DMEM supplemented with 10 mM U-¹³C-glucose and 10% dialyzed FBS and cultured for 6 h. After that, the cells (~1 × 10⁵ cells per sample) were washed twice with saline (pre-warmed at 37 °C) and harvested in 80% methanol aqueous solution.

Metabolite Extraction and Derivatization. Metabolites from the harvested cells were extracted by vigorous vortexing and centrifugation at 22 000*g* for 15 min at 4 °C. The supernatants were evaporated to dryness. Hundred-microliter aliquots of water were used to resolve the dry extracts and then mixed with 50 μL of 175 mM 3-NPH in 75% methanol aqueous solution, 50 μL of 105 mM EDC in methanol, and 50 μL of 2.5% pyridine in methanol. After reaction at 4 °C for 30 min, the mixtures were evaporated to dryness. The dried derivatized metabolites were dissolved in methanol, followed by adding three times volume of water to achieve a final volume of 50 μL.

LC-MS/MS Analysis. Chromatographic separation was performed on a Nexera ultra-high-performance liquid chromatography system (Shimadzu, Kyoto, Japan), with an HSS T3 column (2.1 mm × 150 mm, 1.8 μm, waters) and the following gradient: 0–1.5 min, 5% B; 35.5–36 min, 73–90% B; 39–39.2 min, 90–5% B; and 44 min, 5% B. Mobile phase A was 0.03% formic acid in water. Mobile phase B was 0.03% formic acid in acetonitrile. The flow rate was 0.3 mL/min. The column temperature was kept at 40 °C and the autosampler was kept at 4 °C. The injection volume was 10 μL. Mass data

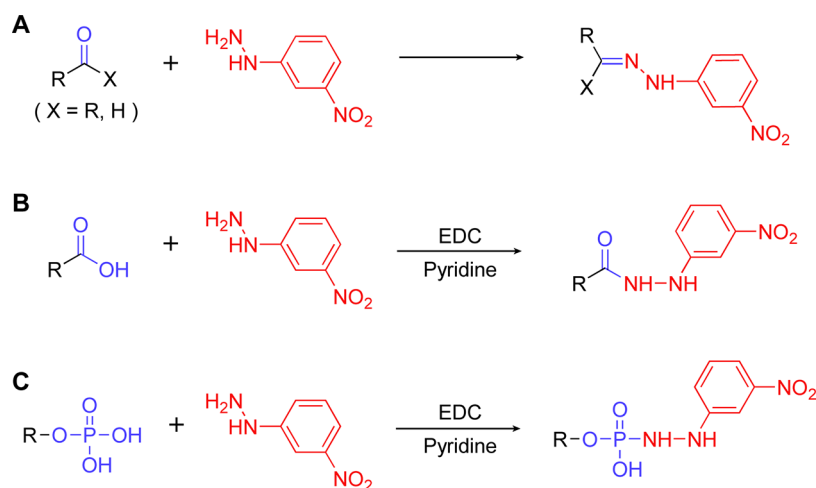


Figure 1. General derivatization schemes for carbonyl (A), carboxyl (B), and phosphoryl (C) groups with 3-NPH.

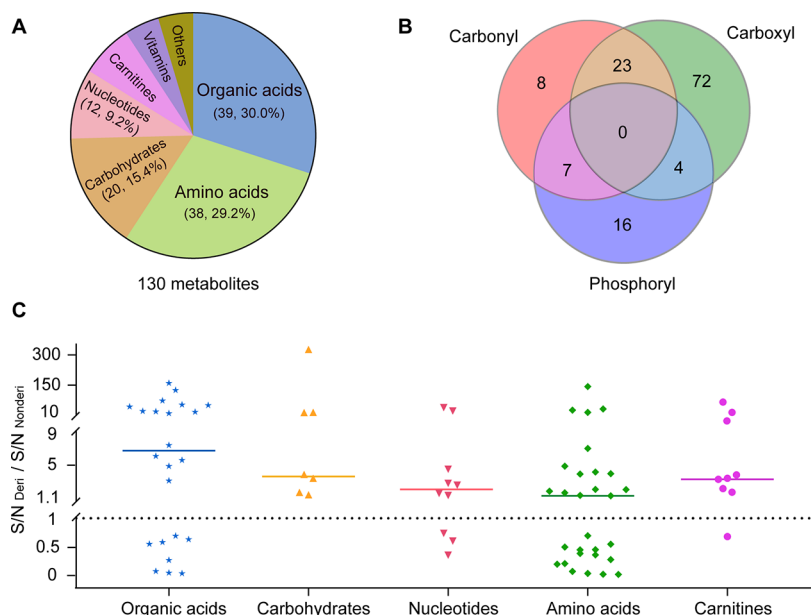


Figure 2. The 3-NPH derivatization strategy improved the detection sensitivity. (A) Overview of the classes of metabolites covered by the method. (B) Numbers of carbonyl-, carboxyl-, and phosphoryl-containing metabolites. (C) Comparison of S/N ratios between 3-NPH-derivatized and nonderivatized metabolites.

acquisition of the 130 derivatized endogenous metabolites was performed using a QTRAP 6500+ mass spectrometer (SCIEX, Framingham, MA) equipped with an electrospray ion source in multiple reaction monitoring (MRM) mode. The parameters of the electrospray ion source were shown in Table S1. The MRM transitions, declustering potential (DP), and collision energy (CE) of all of the derivatized metabolites were shown in Table S2. Metabolite peak review and peak area integration were performed using MultiQuant 3.0.2 (SCIEX, Framingham, MA). The mass isotopomer distribution of each metabolite was calculated after natural abundance correction using IsoCor software.⁴⁷

RESULTS AND DISCUSSION

Derivatization Strategy. Metabolites containing carbonyl, carboxyl, and phosphoryl groups account for a large proportion of the entire metabolome,^{4,35,36,38} including sugars, organic acids, phosphosugars, nucleotides, etc. The simultaneous

analysis of these polar metabolites is of great challenge due to their low ionization efficiency and poor chromatographic retention on the reversed-phase LC column. Chemical derivatization can improve the ionization efficiency and chromatographic retention behavior of metabolites, but the previously reported derivatization methods were mainly developed for one specific group.^{13,35} We aimed to develop a derivatization method that could introduce easily ionizable and hydrophobic moieties into all these three classes of metabolites and allow their simultaneous quantitation in a single LC-MS/MS run. Phenylhydrazine reagents were applied to derivatize the carbonyl group.^{13,45} In addition, the carboxyl group can also be derivatized by phenylhydrazine reagents via nucleophilic addition using a water-soluble carbodiimide, such as EDC, as a coupling reagent.⁴³ Among phenylhydrazine reagents, 3-NPH showed superior reactivity and could produce derivatives with better detection sensitivity.⁴³ Considering the similar reaction mechanism with the carboxyl group, we also tried to use 3-NPH to derivatize phosphoryl-containing

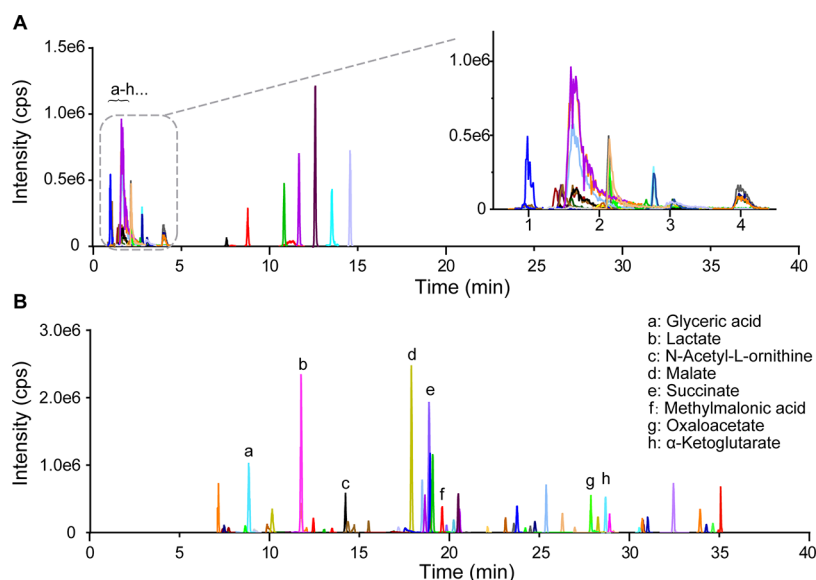


Figure 3. Improved chromatographic separation capability of the 3-NPH derivatization-based method. Extracted ion chromatograms of the nonderivatized metabolites (A) and the derivatized metabolites (B).

metabolites in this study. Phosphorylated metabolites account for a large proportion of the metabolome³⁸ and play a vital role in central carbon and energy metabolism. The derivatization schemes for carbonyl, carboxyl, and phosphoryl groups with 3-NPH were shown in Figure 1. This strategy allowed the simultaneous derivatization of carbonyl, carboxyl, and phosphoryl groups using a single derivatizing reagent, which greatly improved the coverage of the metabolome in a single analysis.

Optimization of Derivatization Conditions. To optimize the derivatization conditions for all the 130 metabolites, and ensure the derivatization method can be applied to the analysis of various biological samples, the concentration of 3-NPH (5, 15, 35, 50, and 70 mM) in the reaction mixture, the reaction time (5, 15, 30, 60, and 120 min), and temperature (4, 10, 25, 30, and 40 °C) were tested in K562 cells, mouse liver, and human plasma by employing previously reported reaction conditions as the starting points.⁴³ The effects of concentration of 3-NPH, reaction time, and temperature on the derivatization of representative metabolites in K562 cells, mouse liver, and human plasma were shown in Figures S1–S3. Based on these results, 35 mM of 3-NPH in the reaction mixture, a reaction temperature of 4 °C, and a reaction time of 30 min were chosen as the optimal conditions.

Under the optimal conditions, for the di- and tricarboxylates, only a small proportion of the partially derivatized products was observed (<5%) and the predominant proportion was the completely derivatized product (>90%), which is consistent with the results previously reported by Han et al.⁴³ Therefore, we chose the completely derivatized products for the quantification of the di- and tricarboxylates. For the multiple phosphates, only the phosphomonoesters were derivatized by 3-NPH, which is consistent with the results reported by Yang et al.⁴⁸

Sensitivity and Separation Capability Improvement.

Based on the 3-NPH derivatization strategy, we developed a highly sensitive LC-MS/MS method that simultaneously targets carbonyl-, carboxyl-, and phosphoryl-containing metabolites for targeted metabolomic analysis. The method covers a total of 130 metabolites, including organic acids, amino acids,

carbohydrates, nucleotides, carnitines, vitamins, and others (Figure 2A). The number of metabolites in each class (carbonyl-, carboxyl-, and phosphoryl-containing class) was shown in Figure 2B. We compared the sensitivity of the derivatization method with that of our previous nonderivatization method¹⁵ by analyzing the metabolome in K562 cells. Figure 2C showed the ratio of the signal-to-noise (S/N) of each metabolite measured by the derivatization method to that measured by the nonderivatization method ($S/N_{\text{Deri}}/S/N_{\text{NonDeri}}$). Overall, the S/Ns of nearly 2/3 of the metabolites improved significantly (2–300 folds) after derivatization (Table S3). Particularly, most of the organic acids, carbohydrates, nucleotides, and carnitines achieved improved sensitivity after derivatization. However, some amino acids and organic acids, such as valine, lysine, and 2,3-pyridinedicarboxylic acid, showed decreased sensitivity after derivatization (Table S3). Given that most of these metabolites present a high ionization efficacy in MS, it is rational to analyze them using our previously reported method without derivatization.¹⁵

By introducing a modifying moiety, the derivatization can convert polar metabolites to their hydrophobic derivatives, which could be efficiently separated on reversed-phase LC columns. Figure 3A,B showed the distributions of the extracted ion chromatograms of metabolites acquired by the nonderivatization and derivatization methods under the same LC condition. Most of the nonderivatized metabolites were co-eluted within 5 min and all of the nonderivatized metabolites were eluted from the column within 15 min (Figure 3A). The derivatized metabolites were gradually eluted from 5 to 35 min and showed good separation (Figure 3B), indicating that the 3-NPH derivatization strategy improved the chromatographic separation. Furthermore, the improved separation allowed the method to separate multiple pairs of isomeric metabolites. Figure S4 showed the nonderivatized and derivatized chromatograms of three representative pairs of isomeric metabolites—glucose and fructose, succinate and methylmalonic acid, and glucose 6-phosphate (G6P) and fructose 6-phosphate (F6P). These difficult-to-discriminate isomers achieved good separation by the derivatization method. This further proved that the derivatization greatly enhanced the

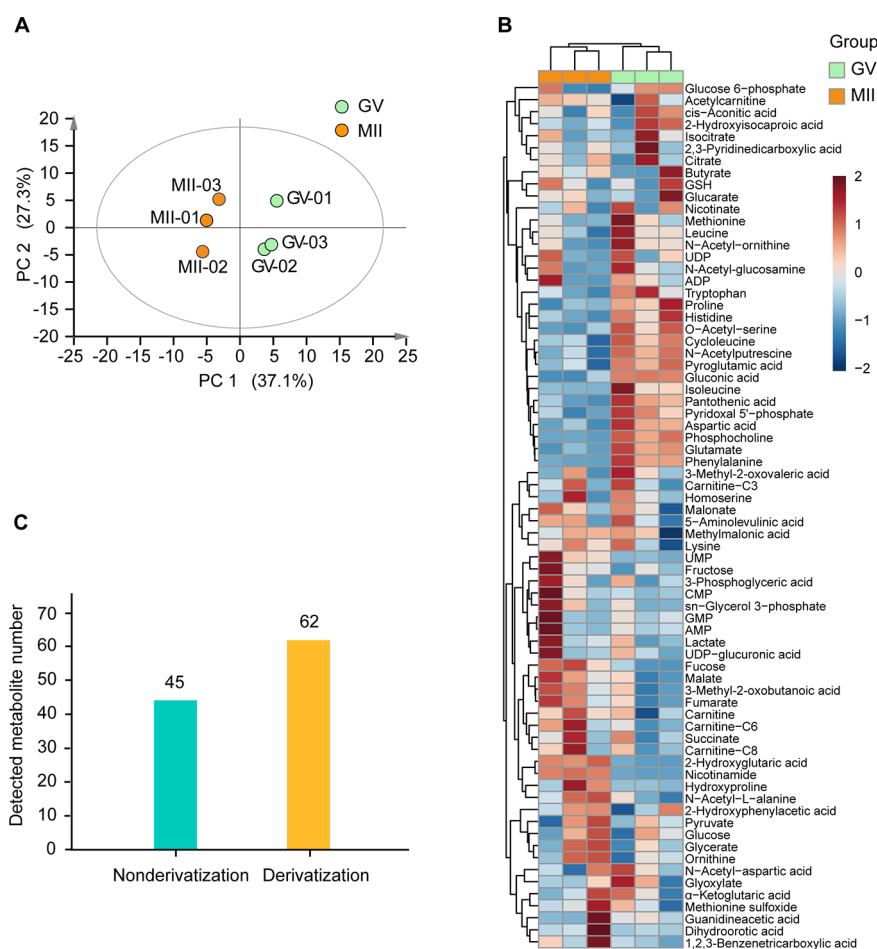


Figure 4. Application of the 3-NPH derivatization strategy for metabolomic analysis of a small number of oocytes and HSCs primarily isolated from mice. (A) PCA plot of mouse oocytes at GV and MII stages ($n = 3$). (B) Heat map of metabolites detected at GV and MII stages ($n = 3$). (C) Comparison of the number of metabolites detected by the nonderivatization method in 5000 HSCs (green) and the 3-NPH derivatization-based method in 5000 HSCs (orange).

separation capability of the metabolomic method and enabled the simultaneous detection of different classes of polar metabolites in a single run.

Limit of Detection (LOD), Lower Limit of Quantification (LOQ), Linearity, and Repeatability. To further validate the 3-NPH derivatization strategy, we evaluated the limit of detection (LOD), the lower limit of quantification (LOQ), linearity, and repeatability of the developed method. The serially diluted standard mixture solutions with concentrations ranging from 0.01 nM to 5 μ M were derivatized and analyzed for the evaluation of LOD, LOQ, and linearity. The results showed that more than 80% of the metabolites showed LODs ≤ 10 nM (Figure S5A). Considering the injection volume was 10 μ L, metabolites that are present in a sample above 100 fmol would be adequate to meet the need for such a metabolomic analysis. Linearity was calculated using a weighted ($1/x^2$) least-squared linear regression method and more than 80% of the metabolites showed a linearity ranging over at least 2 orders of magnitude with regression coefficients of R higher than 0.9. Figure S5B–D showed calibration curves of three representative metabolites, namely glucose (carbonyl-containing metabolite), methylmalonic acid (carboxyl-containing metabolite), and GMP (phosphoryl-containing metabolite). The LODs, LOQs, linear ranges, and regression coefficients (R) of all of the detected metabolites were

shown in Table S4. Repeatability was evaluated by analysis of the extracted K562 cell samples spiked with 100 nM mixed standard solution for six replicates in a single day and three consecutive days. Among the 116 detected metabolites, 114 and 100 metabolites showed good intra-day and inter-day repeatability with a relative standard deviation (RSD) of <20% (Figure S5E), respectively, indicating the method has good repeatability for most of the detected metabolites. The detailed repeatability data was shown in Table S5.

Applications of the 3-NPH Derivatization Method in a Small Number of Oocytes and HSCs. In many metabolism-biology fields such as embryo development and stem cells, only limited amounts of biospecimens are available, which are beyond the sensitivity capability of most current metabolomics technologies. To achieve a decent coverage of the metabolome and for reproducible analysis, researchers usually have to sacrifice hundreds to thousands of mice to collect a sufficient number of primary cells. Takubo et al. pooled $(1-2) \times 10^6$ HSCs from 120 mice for a single metabolomics study.⁴⁹ Li et al. sacrificed 3200 mice and used 2000 oocytes per sample to characterize the metabolic patterns of oocytes during meiotic maturation.¹⁴ Therefore, it urgently necessitates the development of a metabolomics method with high sensitivity that enables the routine metabolomic analysis in trace amounts of biospecimens. To test the utility of the

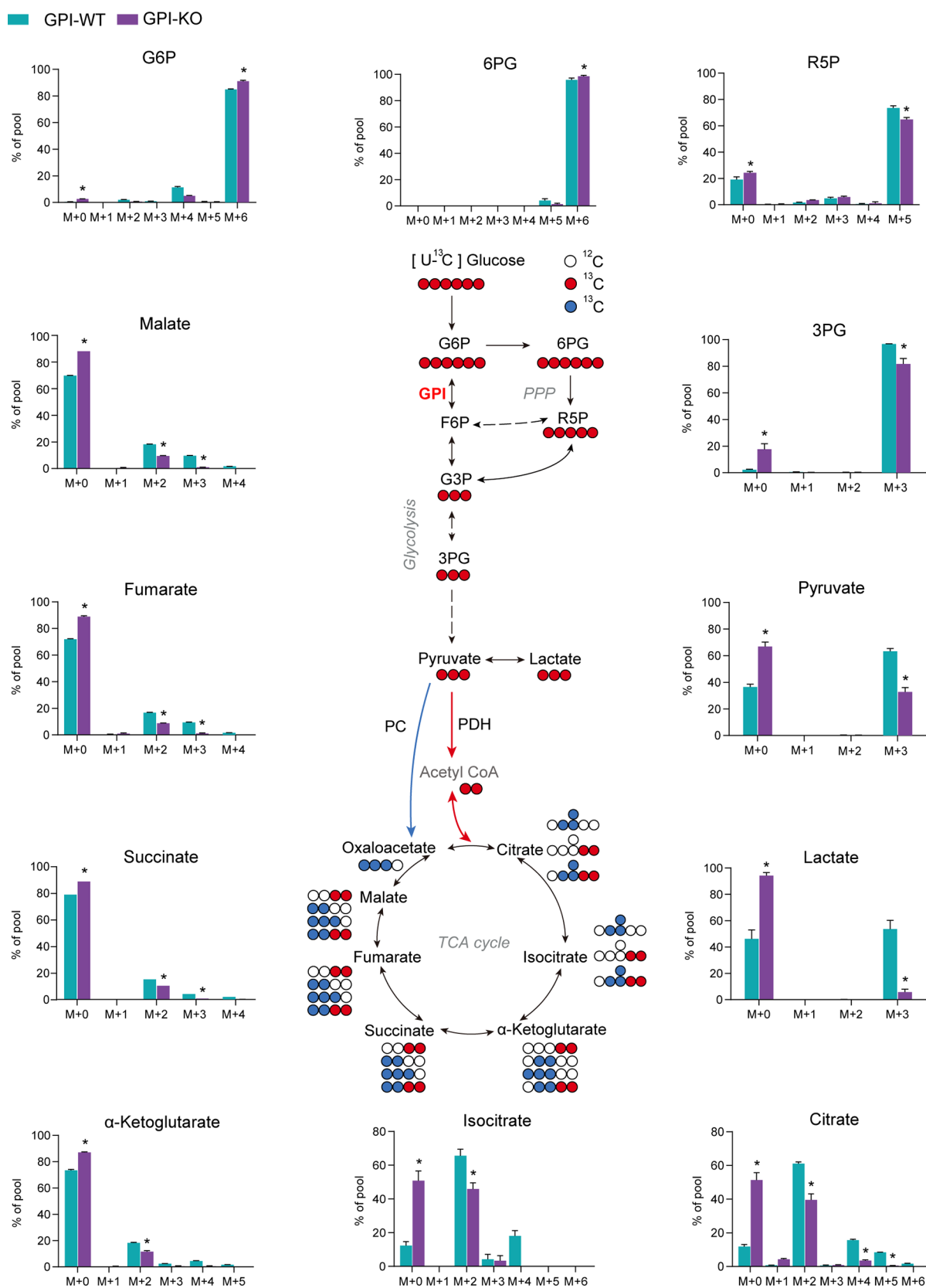


Figure 5. Application of the 3-NPH derivatization method in MFA of glycolysis, the TCA cycle, and PPP. Mass isotopomer distributions of metabolites in GPI-WT and GPI-KO HeLa cells after culture with U-¹³C-glucose for 6 h. The data are displayed as mean ± SD, n = 5. Mann-Whitney U test followed by Benjamini-Hochberg multiple-comparisons test, *p_{adj} < 0.05.

current 3-NPH derivatization-based method in such fields, we applied it to the metabolomic analyses of 60 oocytes and 5000

HSCs primarily isolated from mice. In the mouse oocytes study, metabolomic analysis on the two developmental stages

of oocytes, GV and MII, was performed and 72 out of the 130 monitored metabolites were detected in 60 oocytes. Principal components analysis (PCA) showed that the samples at the same stage clustered well, while samples from the two stages were clearly separated (Figure 4A). The heatmap in Figure 4B showed a similarly distinguished clustering between the two stages of oocytes based on our metabolomics data. Interestingly, the method was also able to detect the subtle variations among different samples in the same stage. In addition, our current 3-NPH derivatization-based method was able to detect 62 out of the 130 monitored metabolites from merely 5000 mouse HSCs. In total, 17 more metabolites were detected when compared to the nonderivatization method in 5000 mouse HSCs (Figure 4C) among which many are functionally important metabolites such as G6P, glyceraldehyde 3-phosphate, and 3-phosphoglyceric acid in glycolysis, and citrate, *cis*-aconitic acid, isocitrate, α -ketoglutarate, and fumarate in the TCA cycle.

These results demonstrated that the developed derivatization strategy-based LC-MS/MS method was highly sensitive and applicable in the metabolomic analysis in trace amounts of biospecimens. When properly expanded to a broader coverage of monitored metabolites, the method could be anticipated to detect even more metabolites.

3-NPH Derivatization Facilitates MFA. The stable isotope labeling-enabled MFA can reflect the directions and turnover rates of metabolites in metabolic pathways and represent the integrated and functional state of metabolism.^{50,51} Isotopologues from an enriched metabolite often have low abundances, which urges a highly sensitive analytical method for detection.⁵² LC-MS/MS operated in MRM mode is highly sensitive and specific for the detection of isotopologues with low abundance. However, for the partial labeling metabolites, the different labeled positions could result in multiple isotopomer patterns for a single isotopologue. Taking α -ketoglutarate as an example (Figure S6A), for a given isotopologue, transitions of each isotopomer are monitored by MRM and summed to obtain the total ion current for this isotopologue.⁵³ This would exponentially increase the number of transitions monitored by MRM in a scan cycle, resulting in decreased detection sensitivity. Moreover, it is necessary and essential to infer the MS/MS fragmentation patterns to obtain the MRM transition of each isotopomer (Figure S6A,B), which makes the analysis much more complex and effort-consuming.

The derivatization strategy can not only improve the sensitivity of the method but also change the MS/MS fragmentation patterns of the metabolites. In this study, we found that many metabolites in glycolysis, the TCA cycle, and PPP pathways generated the common MS/MS fragments derived from the derivatization reagent with high intensity. For carbonyl and carboxyl-containing metabolites, e.g., α -ketoglutarate, it tended to produce the derivatization reagent-specific fragment with m/z 137.0 (Figure S6C). For phosphoryl-containing metabolites, e.g., G6P, it tended to produce a phosphorylated derivatization reagent-specific fragment with m/z 232.0 (Figure S6D). Therefore, for the MFA of glycolysis, the TCA cycle, and PPP, by using the derivatization reagent-specific fragments as fragment ion, only one MRM transition is needed to be monitored for each isotopologue. This greatly reduced the number of MRM transitions that are needed to be monitored and bypassed the tediousness of inferring the MS/MS fragmentation patterns of the metabolites (Figure S6A,B). As a proof-of-concept, we applied this strategy to measure the

mass isotopomer distribution of metabolites in glycolysis, the TCA cycle, and PPP in GPI-WT and GPI-KO HeLa cells cultured with U-¹³C-glucose medium. To investigate the minimum sample amount required for quantification in this labeling study, we performed MFA on different numbers (3×10^4 , 1×10^5 , 3×10^5) of GPI-WT and GPI-KO HeLa cells. Our results demonstrated that the minimum cell number required for this labeling experiment was 1×10^5 with an on-column cell number of 2×10^4 . The rule for the determination of the minimum sample amount is that all of the theoretically produced isotopologues of metabolites in the sample are quantifiable. For example, the M + 2 of isocitrate in the GPI-KO cells showed the lowest abundance and it needed at least 2×10^4 (on-column number) HeLa cells to be quantified. Therefore, we performed this labeling study using 2×10^4 (on-column number) HeLa cells. The percentage of each metabolite isotopologue in Figure 5 and Table S6 showed a relatively decreased metabolic activity toward glycolysis, PPP, and the TCA cycle in GPI-KO cells compared with GPI-WT cells, suggesting that our 3-NPH derivatization-based method can robustly detect the metabolic flux changes between the GPI-WT and GPI-KO HeLa cells. Besides the M + 2 isotopologue, we observed a substantial number of M + 3 and M + 5 isotopologues in the TCA cycle, which may derive from the pyruvate dehydrogenase and pyruvate carboxylase fluxes.^{54,55} Taken together, our results confirmed that the derivatization strategy was suitable for MFA for glycolysis, the TCA cycle, and PPP pathways in cell cultures.

CONCLUSIONS

We presented a derivatization strategy with 3-NPH that simultaneously targets carbonyl-, carboxyl-, and phosphoryl-containing metabolites for LC-MS/MS-based metabolomic analysis with high sensitivity and broad coverage in biological samples. The 3-NPH derivatization provided significantly enhanced sensitivity and chromatographic separation of polar metabolites in the commonly used reversed-phase liquid chromatography. The applicability of the method in trace amounts of biospecimens was demonstrated in 60 oocytes and 5000 HSCs primarily isolated from mice. In addition, we showed that the derivatization strategy facilitated the MFA for glycolysis, the TCA cycle, and PPP in cell cultures. It is anticipated that this novel 3-NPH-based method with high sensitivity, good chromatographic separation, and broad coverage can be widely applied in various metabolism studies, especially for those with trace amounts of biospecimens.

ASSOCIATED CONTENT

Supporting Information

The Supporting Information is available free of charge at <https://pubs.acs.org/doi/10.1021/acs.analchem.1c00767>.

Electrospray ion source parameters (Table S1); MRM transitions, declustering potential (DP) and collision energy (CE) of all the derivatized metabolites (Table S2); Ratios of S/NDeri/S/NNonDeri for all the metabolites (Table S3); LODs, LOQs, linear range and regression coefficients (R) of all the derivatized metabolites (Table S4); Intra-day and inter-day repeatability of the derivatization method (Table S5); Mass isotopomer distribution of metabolites in HeLa cells (Table S6); Effects of different reaction conditions on 3-NPH derivatization of representative metabolites in

K562 cells, human plasma, and mouse liver (Figure S1–S3); Chromatograms of non-derivatized and derivatized three representative pairs of isomeric metabolites (Figure S4); LODs, linearity and repeatability of the 3-NPH derivatization-based method (Figure S5); 3-NPH derivatization strategy facilitates MFA (Figure S6) (PDF)

AUTHOR INFORMATION

Corresponding Author

Zeping Hu – School of Pharmaceutical Sciences, Tsinghua-Peking Joint Center for Life Sciences, Beijing Frontier Research Center for Biological Structure, Tsinghua University, Beijing 100084, China; orcid.org/0000-0003-4146-7750; Email: zeping_hu@tsinghua.edu.cn

Authors

Xiangjun Meng – School of Pharmaceutical Sciences, Tsinghua-Peking Joint Center for Life Sciences, Beijing Frontier Research Center for Biological Structure, Tsinghua University, Beijing 100084, China

Huanhuan Pang – School of Pharmaceutical Sciences, Tsinghua-Peking Joint Center for Life Sciences, Beijing Frontier Research Center for Biological Structure, Tsinghua University, Beijing 100084, China

Fei Sun – School of Pharmaceutical Sciences, Tsinghua-Peking Joint Center for Life Sciences, Beijing Frontier Research Center for Biological Structure, Tsinghua University, Beijing 100084, China

Xiaohan Jin – Department of Biochemistry and Molecular Biology, Capital Medical University, Beijing 100069, China

Bohong Wang – School of Pharmaceutical Sciences, Tsinghua-Peking Joint Center for Life Sciences, Beijing Frontier Research Center for Biological Structure, Tsinghua University, Beijing 100084, China

Ke Yao – School of Pharmaceutical Sciences, Tsinghua-Peking Joint Center for Life Sciences, Beijing Frontier Research Center for Biological Structure, Tsinghua University, Beijing 100084, China

LiAng Yao – School of Pharmaceutical Sciences, Tsinghua-Peking Joint Center for Life Sciences, Beijing Frontier Research Center for Biological Structure, Tsinghua University, Beijing 100084, China

Lijuan Wang – School of Life Sciences, Tsinghua University, Beijing 100084, China

Complete contact information is available at:

<https://pubs.acs.org/10.1021/acs.analchem.1c00767>

Author Contributions

[†]X.M. and H.P. contributed equally to this work. X.M., H.P., and Z.H. conceived the project, designed the study, and wrote the paper. X.M. and F.S. developed the method and collected the experimental data. H.P. and X.M. designed and performed the metabolic flux experiment. B.W. and K.Y. assisted in the method development. X.J., L.Y., and L.W. assisted in the metabolomics experiments. All authors have given approval to the final version of the manuscript. Z.H. supervised the project.

Notes

The authors declare no competing financial interest.

ACKNOWLEDGMENTS

We appreciate Dr. Binghui Li for providing the HeLa cells, Drs. Jianwei Wang and Min Liao for providing HSCs and K562 cells, and Drs. Wei Xie and Shuyan Ji for providing oocytes. We thank the members of the Hu laboratory for critiquing the manuscript. Z.H. is supported by grants from the National Natural Science Foundation of China (92057209), National Key R&D Program of China (2019YFA0802100-02, 2020YFA0803300), National Science and Technology Major Project for “Significant New Drugs Development” (2017ZX09304015), Tsinghua University (53332200517), Tsinghua-Peking Joint Center for Life Sciences, and Beijing Frontier Research Center for Biological Structure.

REFERENCES

- (1) Li, Y.; Bouza, M.; Wu, C.; Guo, H.; Huang, D.; Doron, G.; Temenoff, J. S.; Stecenko, A. A.; Wang, Z. L.; Fernández, F. M. *Nat. Commun.* **2020**, *11*, No. 5625.
- (2) Newgard, C. B. *Cell Metab.* **2017**, *25*, 43–56.
- (3) Chen, Y.; Zhou, Z.; Yang, W.; Bi, N.; Xu, J.; He, J.; Zhang, R.; Wang, L.; Abliz, Z. *Anal. Chem.* **2017**, *89*, 6954–6962.
- (4) Zhao, S.; Li, H.; Han, W.; Chan, W.; Li, L. *Anal. Chem.* **2019**, *91*, 12108–12115.
- (5) Chaleckis, R.; Meister, I.; Zhang, P.; Wheelock, C. E. *Curr. Opin. Biotechnol.* **2019**, *55*, 44–50.
- (6) Sindelar, M.; Patti, G. J. *J. Am. Chem. Soc.* **2020**, *142*, 9097–9105.
- (7) Petucci, C.; Zelenin, A.; Culver, J. A.; Gabriel, M.; Kirkbride, K.; Christison, T. T.; Gardell, S. J. *Anal. Chem.* **2016**, *88*, 11799–11803.
- (8) Iturraspe, E.; Da Silva, K. M.; Talavera Andújar, B.; Cuykx, M.; Boeckmans, J.; Vanhaecke, T.; Covaci, A.; van Nuijs, A. L. N. *J. Chromatogr. A* **2021**, *1637*, No. 461807.
- (9) Cifuentes Girard, M. F.; Ruskic, D.; Bohm, G.; Picononi, R.; Hopfgartner, G. *Anal. Chim. Acta* **2020**, *1127*, 198–206.
- (10) Xhaferaj, M.; Naegele, E.; Parr, M. K. *J. Chromatogr. A* **2020**, *1614*, No. 460726.
- (11) Berthias, F.; Wang, Y.; Alhaji, E.; Rieul, B.; Moussa, F.; Benoist, J. F.; Maître, P. *Analyst* **2020**, *145*, 4889–4900.
- (12) Sarvin, B.; Lagziel, S.; Sarvin, N.; Mukha, D.; Kumar, P.; Aizenshtein, E.; Shlomi, T. *Nat. Commun.* **2020**, *11*, No. 3186.
- (13) Siegel, D.; Meinema, A. C.; Permentier, H.; Hopfgartner, G.; Bischoff, R. *Anal. Chem.* **2014**, *86*, 5089–5100.
- (14) Li, L.; Zhu, S.; Shu, W.; Guo, Y.; Guan, Y.; Zeng, J.; Wang, H.; Han, L.; Zhang, J.; Liu, X.; Li, C.; Hou, X.; Gao, M.; Ge, J.; Ren, C.; Zhang, H.; Schedl, T.; Guo, X.; Chen, M.; Wang, Q. *Mol. Cell* **2020**, *80*, 525–540.e529.
- (15) Agathocleous, M.; Meacham, C. E.; Burgess, R. J.; Piskounova, E.; Zhao, Z.; Crane, G. M.; Cowin, B. L.; Bruner, E.; Murphy, M. M.; Chen, W.; Spangrude, G. J.; Hu, Z.; DeBerardinis, R. J.; Morrison, S. J. *Nature* **2017**, *549*, 476–481.
- (16) O'Brien, K. L.; Finlay, D. K. *Nat. Rev. Immunol.* **2019**, *19*, 282–290.
- (17) DeNicola, G. M.; Chen, P. H.; Mullarky, E.; Sudderth, J. A.; Hu, Z.; Wu, D.; Tang, H.; Xie, Y.; Asara, J. M.; Huffman, K. E.; Wistuba, I. I.; Minna, J. D.; DeBerardinis, R. J.; Cantley, L. C. *Nat. Genet.* **2015**, *47*, 1475–1481.
- (18) Huang, F.; Ni, M.; Chalisehar, M. D.; Huffman, K. E.; Kim, J.; Cai, L.; Shi, X.; Cai, F.; Zacharias, L. G.; Ireland, A. S.; Li, K.; Gu, W.; Kaushik, A. K.; Liu, X.; Gazdar, A. F.; Oliver, T. G.; Minna, J. D.; Hu, Z.; DeBerardinis, R. J. *Cell Metab.* **2018**, *28*, 369–382.e365.
- (19) Kim, J.; Hu, Z.; Cai, L.; Li, K.; Choi, E.; Faubert, B.; Bezwada, D.; Rodriguez-Canales, J.; Villalobos, P.; Lin, Y. F.; Ni, M.; Huffman, K. E.; Girard, L.; Byers, L. A.; Unsal-Kacmaz, K.; Peña, C. G.; Heymach, J. V.; Wauters, E.; Vansteenkiste, J.; Castrillon, D. H.; et al. *Nature* **2017**, *546*, 168–172.

- (20) Piskounova, E.; Agathocleous, M.; Murphy, M. M.; Hu, Z.; Huddleston, S. E.; Zhao, Z.; Leitch, A. M.; Johnson, T. M.; DeBerardinis, R. J.; Morrison, S. J. *Nature* **2015**, *527*, 186–191.
- (21) Shi, X.; Tasdogan, A.; Huang, F.; Hu, Z.; Morrison, S. J.; DeBerardinis, R. J. *Sci. Adv.* **2017**, *3*, No. eaao5268.
- (22) Srivastava, N.; Kollipara, R. K.; Singh, D. K.; Sudderth, J.; Hu, Z.; Nguyen, H.; Wang, S.; Humphries, C. G.; Carstens, R.; Huffman, K. E.; DeBerardinis, R. J.; Kittler, R. *Cell Metab.* **2014**, *20*, 650–661.
- (23) Xiang, J.; Chen, C.; Liu, R.; Gou, D.; Chang, L.; Deng, H.; Gao, Q.; Zhang, W.; Tuo, L.; Pan, X.; Liang, L.; Xia, J.; Huang, L.; Yao, K.; Wang, B.; Hu, Z.; Huang, A.; Wang, K.; Tang, N. *J. Clin. Invest.* **2021**, *131*, No. e144703.
- (24) Li, X.-K.; Lu, Q.-B.; Chen, W.-W.; Xu, W.; Liu, R.; Zhang, S.-F.; Du, J.; Li, H.; Yao, K.; Zhai, D.; Zhang, P.-H.; Xing, B.; Cui, N.; Yang, Z.-D.; Yuan, C.; Zhang, X.-A.; Xu, Z.; Cao, W.-C.; Hu, Z.; Liu, W. *Sci. Transl. Med.* **2018**, *10*, No. eaat4162.
- (25) Xiao, N.; Nie, M.; Pang, H.; Wang, B.; Hu, J.; Meng, X.; Li, K.; Ran, X.; Long, Q.; Deng, H.; Chen, N.; Li, S.; Tang, N.; Huang, A.; Hu, Z. *Nat. Commun.* **2021**, *12*, No. 1618.
- (26) Liu, X.; Zhang, Y.; Ni, M.; Cao, H.; Signer, R. A. J.; Li, D.; Li, M.; Gu, Z.; Hu, Z.; Dickerson, K. E.; Weinberg, S. E.; Chandel, N. S.; DeBerardinis, R. J.; Zhou, F.; Shao, Z.; Xu, J. *Nat. Cell Biol.* **2017**, *19*, 626–638.
- (27) Nakada, Y.; Canseco, D. C.; Thet, S.; Abdisalaam, S.; Asaithamby, A.; Santos, C. X.; Shah, A. M.; Zhang, H.; Faber, J. E.; Kinter, M. T.; Szweda, L. I.; Xing, C.; Hu, Z.; Deberardinis, R. J.; Schiattarella, G.; Hill, J. A.; Oz, O.; Lu, Z.; Zhang, C. C.; Kimura, W.; et al. *Nature* **2017**, *541*, 222–227.
- (28) Zhu, X.; Shen, W.; Yao, K.; Wang, H.; Liu, B.; Li, T.; Song, L.; Diao, D.; Mao, G.; Huang, P.; Li, C.; Zhang, H.; Zou, Y.; Qiu, Y.; Zhao, Y.; Wang, W.; Yang, Y.; Hu, Z.; Auwerx, J.; Loscalzo, J.; et al. *Circ. Res.* **2019**, *125*, 707–719.
- (29) Vuckovic, D. *Chem. Commun.* **2018**, *54*, 6728–6749.
- (30) Higashi, T.; Ogawa, S. *J. Chromatogr. A* **2020**, *1634*, No. 461679.
- (31) Zhang, H.; Shi, X.; Vu, N. Q.; Li, G.; Li, Z.; Shi, Y.; Li, M.; Wang, B.; Welham, N. V.; Patankar, M. S.; Weisman, P.; Li, L. *Anal. Chem.* **2020**, *92*, 13361–13368.
- (32) Hao, L.; Johnson, J.; Lietz, C. B.; Buchberger, A.; Frost, D.; Kao, W. J.; Li, L. *Anal. Chem.* **2017**, *89*, 1138–1146.
- (33) Zhao, S.; Luo, X.; Li, L. *Anal. Chem.* **2016**, *88*, 10617–10623.
- (34) Peng, J.; Li, L. *Anal. Chim. Acta* **2013**, *803*, 97–105.
- (35) Zhao, S.; Li, L. *Anal. Chem.* **2018**, *90*, 13514–13522.
- (36) Zhao, S.; Dawe, M.; Guo, K.; Li, L. *Anal. Chem.* **2017**, *89*, 6758–6765.
- (37) Chen, D.; Yu, J.; Zhang, Z.; Su, X.; Li, L.; Li, L. *Anal. Chem.* **2019**, *91*, 4958–4963.
- (38) Uehara, T.; Yokoi, A.; Aoshima, K.; Tanaka, S.; Kadowaki, T.; Tanaka, M.; Oda, Y. *Anal. Chem.* **2009**, *81*, 3836–3842.
- (39) Deng, P.; Higashi, R. M.; Lane, A. N.; Bruntz, R. C.; Sun, R. C.; Ramakrishnam Raju, M. V.; Nantz, M. H.; Qi, Z.; Fan, T. W. *Analyst* **2018**, *143*, 311–322.
- (40) Jin, Y.-Y.; Shi, Z.-Q.; Chang, W.-Q.; Guo, L.-X.; Zhou, J.-L.; Liu, J.-Q.; Liu, L.-F.; Xin, G.-Z. *J. Pharm. Biomed. Anal.* **2018**, *161*, 336–343.
- (41) Han, J.; Higgins, R.; Lim, M. D.; Atkinson, K.; Yang, J.; Lin, K.; Borchers, C. H. *Anal. Chim. Acta* **2018**, *1037*, 177–187.
- (42) Han, J.; Lin, K.; Securia, C.; Yang, J.; Borchers, C. H. *Electrophoresis* **2016**, *37*, 1851–1860.
- (43) Han, J.; Gagnon, S.; Eckle, T.; Borchers, C. H. *Electrophoresis* **2013**, *34*, 2891–2900.
- (44) Zimmermann, M.; Sauer, U.; Zamboni, N. *Anal. Chem.* **2014**, *86*, 3232–3237.
- (45) Lattová, E.; Perreault, H. *Mass Spectrom. Rev.* **2013**, *32*, 366–385.
- (46) DeVilbiss, A. W.; Zhao, Z.; Martin-Sandoval, M. S.; Ubellacker, J. M.; Tasdogan, A.; Agathocleous, M.; Mathews, T. P.; Morrison, S. J. *Life* **2021**, *10*, No. e61980.
- (47) Millard, P.; Letisse, F.; Sokol, S.; Portais, J. C. *Bioinformatics* **2012**, *28*, 1294–1296.
- (48) Yang, W.-C.; Sedlak, M.; Regnier, F. E.; Mosier, N.; Ho, N.; Adamec, J. *Anal. Chem.* **2008**, *80*, 9508–9516.
- (49) Takubo, K.; Nagamatsu, G.; Kobayashi, C. I.; Nakamura-Ishizu, A.; Kobayashi, H.; Ikeda, E.; Goda, N.; Rahimi, Y.; Johnson, R. S.; Soga, T.; Hirao, A.; Suematsu, M.; Suda, T. *Cell Stem Cell* **2013**, *12*, 49–61.
- (50) Badur, M. G.; Metallo, C. M. *Metab. Eng.* **2018**, *45*, 95–108.
- (51) Long, C. P.; Antoniewicz, M. R. *Nat. Protoc.* **2019**, *14*, 2856–2877.
- (52) Shi, X.; Xi, B.; Jasbi, P.; Turner, C.; Jin, Y.; Gu, H. *Anal. Chem.* **2020**, *92*, 11728–11738.
- (53) Yuan, M.; Kremer, D. M.; Huang, H.; Breitkopf, S. B.; Ben-Sahra, I.; Manning, B. D.; Lyssiotis, C. A.; Asara, J. M. *Nat. Protoc.* **2019**, *14*, 313–330.
- (54) Williams, H. C.; Farmer, B. C.; Piron, M. A.; Walsh, A. E.; Bruntz, R. C.; Gentry, M. S.; Sun, R. C.; Johnson, L. A. *Neurobiol. Dis.* **2020**, *136*, No. 104742.
- (55) Alves, T. C.; Pongratz, R. L.; Zhao, X.; Yarborough, O.; Sereda, S.; Shirihai, O.; Cline, G. W.; Mason, G.; Kibbey, R. G. *Cell Metab.* **2015**, *22*, 936–947.